DEVELOPMENT OF LIMB-SCATTERING RADIATIVE TRANSFER MODELS FOR MARS REMOTE SENSING AND DATA ASSIMILATION. J. Eluszkiewicz[1], D. E. Flittner[2], J.-L. Moncet[1], and M. J. Wolff[3], [1]Atmospheric and Environmental Research, Inc., 131 Hartwell Ave., Lexington, MA 02421, jel@aer.com, [2]NASA Langley Research Center, [3]Space Science Institute.

Introduction: Measurements of the martian atmosphere have experienced rapid growth during the past decade. As on Earth, remote sensing from orbit offers the advantage of nearly continuous, global coverage and a host of instruments have been employed for this purpose, including cameras [the Mars Orbiter Camera (MOC) and the Mars Color Imager (MARCI)] and infrared sounders [the Thermal Emission Spectrometer (TES), the Mars Climate Sounder (MCS), and Compact Reconnaissance Imaging Spectrometer for Mars (CRISM)], as well as European instruments. The MCS is a dedicated atmospheric instrument, while the other instruments have yielded a wealth of information about the atmosphere in addition to their primary surface-studies focus.

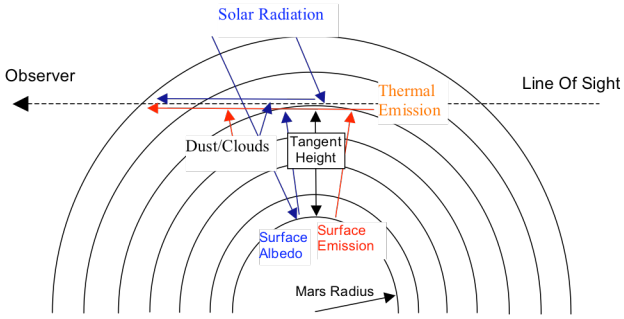

Figure 1: The limb-viewing geometry. The radiances measured by the observer come from the Sun (e.g., cameras, CRISM) or thermal emission (MCS, TES).

From the point of view of atmospheric studies, the dedicated limb-observing capability of the MCS, as well as the limb viewing "of opportunity" afforded by the TES, MOC, MARCI, and CRISM instruments offer significant advantages compared with the nadir-viewing mode. The geometry of limb measurements is illustrated in Figure 1. Chief among the advantages are the improved vertical resolution (particularly relevant to the studies of dynamic phenomena as reflected in the thermal structure) and the fact that observing against a cold space background (as opposed to a warm surface) offers the possibility of retrieving vertically resolved information about aerosols (including dust and H_2O and CO_2 ices) and minor gases (water vapor, carbon monoxide, etc.). The main limitation to attaining the full scientific potential of limb measurements is the general lack of appropriate radiative transfer models. Such models must be capable, in a computationally efficient manner suitable for retrieval and radiance assimilation work, of accurately representing both gaseous absorption and aerosol scattering in a spherical geometry. The ubiquitous nature of aerosols in the martian atmosphere enhances the importance of scattering for limb viewing geometry (versus that of nadir), e.g., a normal optical depth of 0.4 produces a line of sight optical depth of approximately 3 and 7 for tangent point altitudes 20 km and 10 km, respectively. These numbers assume that the aerosols are uniformly mixed (with a scale height of 10 km). In fact, there is evidence that suggests that dust is actually more confined during lower opacity periods [1]. As a result, the slant optical depths increase even more towards lower tangent points, further complicating limb retrievals of the lower atmosphere. An optimal solution to this problem would employ a combination of limb and off-nadir measurements, particularly the emergence phase function (EPF) observations by CRISM [2].

Given the above considerations, we have recently commenced work on developing rigorous radiative transfer models capable of simulating limb radiances in the presence of gaseous absorption and scattering. Our work has two overarching purposes. The first is to establish a set of rigorous benchmark calculations against which approximate methods to the limb absorption+scattering problem [3, 4] can be validated. These calculations will be carried out using a fully spherical limb code [5, 6] for scattering and the line-by-line model LBLRTM [7] for gaseous absorption. The second objective is to develop a fast parameterization capable of accurately and efficiently calculating limb radiances in the presence of gaseous absorption and scattering by aerosols. At the heart of this parameterization lies the Optimal Sampling Method (OSS) for gaseous absorption [8] that has been specifically designed to reproduce the accuracy of LBL calculations, but at a miniscule fraction of the computational cost. The OSS method treats gaseous absorption in a monochromatic way, making it a natural choice for coupling to a scattering code. The OSS-based parameterizations will be developed separately for the MCS, TES, and CRISM instruments (in the latter case including both the limb and EPF geometries), while a purely scattering version of the code will be adopted to model the MARCI limb measurements. This suite of models tailored to four instruments will provide a fertile ground for various cross-validation studies spanning the visible, near-IR, and thermal IR spectral regions.

Limb-Scattering Model: The scattering radiative transfer model (RTM) chosen for this project, the Gauss Seidel Spherical RTM (GSSRTM) [5,6], has

been in use for nearly 20 years. Scattering by molecules, dust, and clouds (with phase functions following Mie theory or any tabulated form) is computed. The model is monochromatic in nature and computes all orders of scattering in a completely spherical atmosphere. For the work described here, the polarization of scattered light is neglected with very little loss in accuracy (mainly because Rayleigh scattering is small and aerosols are expected to be randomly oriented). This leads to a significant reduction in run-time when compared to the polarized GSSRTM. The model is fully spherical in the sense that all path lengths (including those for multiple scattering) are for a spherical atmosphere. The GSSRTM can be run in a line-by-line fashion over spectral features (see Figure 3 below).

LBL Calculations of Gaseous Absorption: In both the benchmarking and parameterization portions of our work, the LBLRTM model [7] provides the line-by-line calculations of optical depths due to gaseous absorption, giving us direct access to on-going radiance closure studies [9] and enabling the model to be quickly and rigorously updated as our knowledge of the fundamental spectroscopic parameters improves. Recently, we have enhanced the capabilities of the LBLRTM code specifically for the development of GCM-suitable radiation codes for studies of the climate of paleo-Earth, -Mars, and other terrestrial planets, with two of these upgrades directly relevant to the work described herein. First, newly calculated CO_2-broadened line parameters (half-widths, line shifts, and temperature dependence of widths) of water vapor lines [10, 11] have been incorporated. Since these calculations did not cover numerous water vapor lines of interest, we developed a scheme to estimate the CO_2-broadened line parameters of these lines. Second, the water vapor continuum model MT_CKD [7] has been adjusted to account for differences between air- and CO_2-broadening of water vapor lines and their relative efficiency in generating collision-induced absorption. These two modifications result in a change of 10-20% in the retrieved column water vapor under current martian conditions (compared to calculations employing the more basic modifications described in [12]), with most of this difference stemming from changes to the water vapor continuum.

Example: In order to illustrate the performance of the limb scattering model in the presence of both gaseous absorption and aerosol scattering, we have computed LBL spectra in the 200-300 cm^{-1} spectral region that encompasses the MCS B2 and B3 bands as well as several TES channels. The main source of gas absorption in this spectral range are the rotational lines of water vapor, for which we assumed a constant mixing ratio of 150 ppmv. The optical depths due to absorption by water vapor have been computed using the LBLRTM code, adapted to Mars as described above. For dust, we assumed a normal optical depth for extinction of 1 at 9.3 μm and uniform mixing. The absorption and scattering optical depths and asymmetry parameter in the 200-300 cm^{-1} region have been calculated using Mie indices derived for martian dust [1]. The atmospheric inputs to our calculations are plotted in Figure 2.

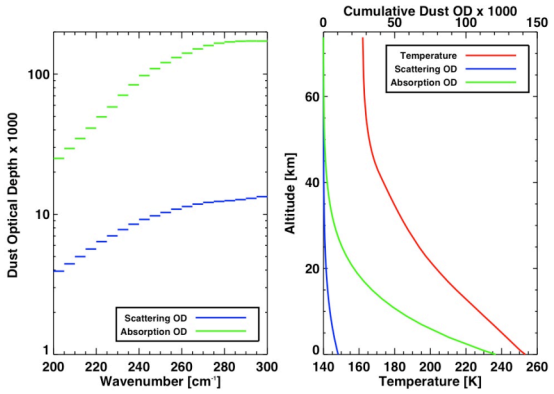

Figure 2: Left: Column (normal) dust optical depth as a function of wavenumber employed in the sample calculationsRight: Cumulative (normal) dust optical depth at 250 cm^{-1} and temperature as a function of altitude.

The upper panel of Figure 3 shows monochromatic radiances computed using the GSSRTM code in its fully scattering mode, illustrating the kind of benchmark cases our work will generate. The lower panel of Figure 3 presents errors (in percent) stemming from the neglect of scattering, computed as percentage differences (relative to the fully scattering case) between calculations employing the non-scattering and fully scattering versions of the GSSRTM code. Several features in Figure 3 are noteworthy. The enhanced radiance levels correspond to strong water lines. In these spectral "micro-windows" scattering is unimportant, as evidenced by the vanishing differences between the purely absorbing and fully scattering cases. However, over most of the spectral range shown in Figure 3, scattering leads to significantly enhanced radiances compared with the non-scattering case and has a large impact on the spectrally broad channel radiances (see Figure 4 below). The largest enhancements of more than 10% occur at tangent heights above 30 km, above the level of highest opacity (see Figure 2) and reflect radiance emitted at lower altitudes and scattered into the line-of-sight. Interestingly, the impact of scattering decreases towards shorter wavelengths/larger wavenumbers, despite the fact that scattering opacity increases with decreasing wavelengths (see Figure 2). This is due to the fact that the absorption opacity increases more rapidly towards shorter wavelengths than

scattering opacity and this dampens the relative contribution from scattering (for this reason, the absolute radiances in the upper panel of Figure 2 increase towards shorter wavelengths). Apart from the lowest 5 km and the strong water vapor lines, the percentage differences shown in Figure 3 greatly exceed the MCS absolute radiometric calibration requirement of better than 0.5% [13]. These results strongly suggest that scattering must be included in the modeling of instrument channels located in this spectral region and our tools will accomplish this in a rigorous way. The spectral region in this example has been chosen because it includes strong gaseous absorption, the modeling of which is central to the our work. However, the scattering opacity of the assumed martian dust is relatively low in this spectral range (see Figure 2). Consequently, we expect that the importance of scattering will increase towards shorter wavelengths (e.g., the CRISM near-IR channels). Furthermore, the percentage differences shown in Figure 3 do not reflect other sources of errors, e.g., those stemming from a less rigorous treatment of spherical geometry. The discontinuities at 5 cm^{-1} intervals evident in Figure 3 (particularly pronounced at 235 and 240 cm^{-1}, two wavenumbers with small gaseous absorption) are an artifact of assuming that dust optical properties are constant across these intervals (see Figure 2). Currently, we are adopting a more realistic approach in which these properties are interpolated to the monochromatic frequencies.

By convolving LBL radiances such as those shown in Figure 3 with the instrument spectral response function, the channel or band radiances for a particular instrument can be computed. Figure 4 shows examples of synthetic radiances for two TES channels and the MCS B3 band (the convolution over each instrument's finite field-of-view has been neglected). The impact of scattering is evident, with errors incurred by ignoring it on the order of several percent. Because of the proximity to strong water lines (where scattering is less important) and owing to the relative importance of absorption and scattering discussed above, these errors are smaller (but significant) for the TES channel at 254.7 cm^{-1} (compared to the channel at 233.8 cm^{-1}). Furthermore, errors caused by the neglect of scattering maximize at heights above the bulk of dust opacity.

Fast RTM: "Brute force" monochromatic calculations of channel radiances are clearly impractical for operational applications. A standard approach to this problem is to develop a "fast" radiative transfer model. In our work, a fast RTM for a spherical scattering and absorbing atmosphere will be developed in three steps: 1) Reducing the LBL problem for gaseous absorption to a limited number of monochromatic calculations that reproduce the LBL calculations to within a pre-set accuracy 2) Performing scattering calculations at the selected monochromatic frequencies over a wide range of conditions, and 3) Development of look-up tables for use in retrieval and radiance assimilation, based on the calculations performed in Step 2). Step 1) consists in the modeling of the spectra using the OSS method [8], in which channel radiances are approximated as linear combinations of radiances computed at selected monochromatic locations. The OSS spectral locations and their statistical weights are selected by comparing the resulting channel radiances against LBL calculations performed over a wide range of atmospheric profiles. These "training" profiles are chosen to be representative of the expected variability, including atmospheric temperature and composition, aerosol distribution and optical properties, surface pressure, surface emissivity and reflectivity, and viewing and solar angles. Accurate and computationally efficient modeling of scattering effects employs the GSSRTM code at the OSS frequencies and we refer to this combined model as the "OSS-LimbScat" model.

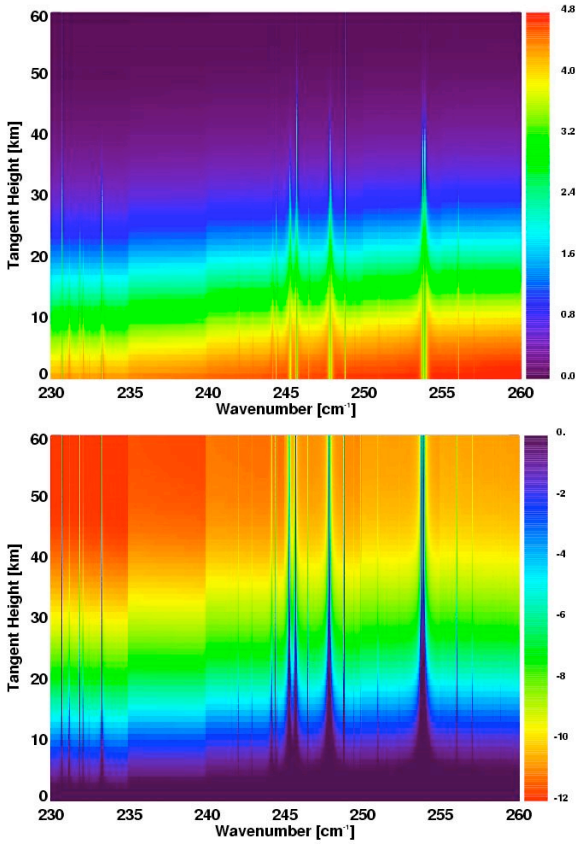

Figure 3: Upper panel: LBL radiances in the 230-260 cm^{-1} spectral range as a function of tangent height computed using the the GSSRTM code. Units are 100 x $W/m^2/cm^{-1}/sr$. Lower panel: Errors due to the neglect of scattering, computed as percentage differences between radiances employing the absorption-only and fully scattering versions of the GSSRTM code.

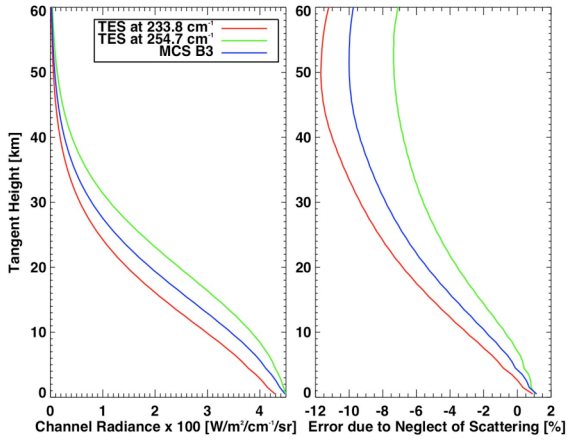

Figure 4: Synthetic radiances for two TES channels and the MCS B3 band. The left panel shows the absolute fully scattering radiances and the right panel the errors stemming from the neglect of scattering.

Once the training set is constructed, the next step in OSS training are radiance calculations using the LBLRTM/GSSRTM code. For down-looking sensors in the thermal infrared, this is usually done under clear-sky assumptions, as long as spectral variations in cloud optical properties across channel bandwidth are not significant. However, the clear-sky assumption is not adequate in the limb case, where a straightforward line-of-sight path is very different from the path encountered when scattering is important (in the latter case, in addition to photons coming directly from the line of sight, the observer sees photons that come from the generally warmer layers and surface below the tangent altitude and are scattered into the line of sight, see Figure 1). In order to deal with this conundrum, we plan to employ "brute-force" LBL calculations in the fully scattering mode. In addition to including variable tangent height in the training, the training set will also allow for variability in the viewing angle, for the purpose of generating a forward model for the CRISM EPF sequences. For CRISM, the OSS model will be trained mainly for channels with absorption due to CO_2 and H_2O (e.g., at 2.6 μm). Channels where other gases absorb (e.g., CO) will be considered at a later stage if a suitable training set for those gases can be identified.

The final step in the OSS training is the node selection that employs a search method to find "optimal" frequencies and their weights that approximate the rigorous LBL-based channel radiances over the entire training set to within a prescribed level of accuracy (typically set to better than the instrument noise level, e.g., 0.05 K). The various procedures for the selection step are described in [8] and, since the selection is performed in the radiance space, they are quite general regardless of the viewing geometry.

"Super-Fast" Parameterization: The OSS-LimbScat model will perform scattering calculations on the selected monochromatic frequencies. Preliminary timing estimates indicate that for 100 OSS nodes (a number that we expect to be sufficient for the eight MCS channels relevant for retrieval work, excluding the broadband A6 channel), the fully scattering calculations will take approximately 30 seconds/profile on one processor of a modern desktop computer. This represents a tremendous speed increase (by a factor of 10^3-10^4) compared with brute-force LBL scattering calculations and puts the model in the "ball-park" of speed requirements for an operational code. However, it is possible (in fact, likely) that this direct approach will still fall short of the timing requirements for an operational processing of MCS and TES spectra, both in data-assimilation and retrievals. Consequently, we plan to develop a "super-fast" parameterization for operational use. Guided by our terrestrial work [e.g., 14], our approach aimed at operational speed will consist of splitting the scattering calculation into a single-scatter calculation and a correction for multiple scattering expressed as a look-up table. The independent variables in the table will be the total opacity of aerosols, their particle size (or scattering properties, e.g., single-scattering albedo), and total water vapor column. The look-up table will be constructed using the LBL scattering calculations performed as part of OSS training, augmented by calculations utilizing the OSS-LimbScat model extending over a wider range of conditions. Besides the look-up table for multiple scattering, our approach to super-fast parameterization will also include the so-called "scattering accelerator," in which the scattering calculations are performed at a small number of OSS nodes (typically 2-3 per channel) and the calculations at the remaining nodes are expressed by means of statistical regression against the "fully-scattering" nodes. This will be implemented directly in the radiance space (using the LBL radiances as a benchmark) and the mathematical techniques are the same as those developed for the nadir case.

References: [1] Wolff M. J. et al. (2006) *J. Geophys. Res., 111,* E12S17. [2] Murchie S. et al. (2007), *J. Geophys. Res.*, *112*, E05S03. [3] Kleinböhl A. et al. (2008), Mars Water Cycle Workshop, Paris. [4] Smith M. D. (2003) 6th Mars Conference, Abstract #3174. [5] Herman B. M. et al. (1994) *Appl. Opt., 33,* 1760. [6] Herman B. M. et al. (1994) *Appl. Opt., 34,* 4563. [7] Clough S. A. et al. (2005) *JQSRT*, *91,* 233. [8] Moncet J.-L. et al. (2008) *J. Atmos. Sci.* (in press). [9] Turner D. D. et al. (2004) *J. Atmos. Sci., 61,* 2,657. [10] R. Gamache (2008) personal comm. [11] Brown L. R. et al. (2007) *J. Mol. Spectrosc., 246,* 1. [12] Smith M. D. (2002) *J. Geophys. Res., 107,* 5115. [13] McCleese D. J. et al. (2007) *J. Geophys. Res., 112,* E05S06. [14] Flittner D. E. et al. (2000) *Geophys. Res. Lett., 27,* 2601.